Light reflection induced changes in the line shape of sputtered atoms

S. Ertmer, O. Marchuk, S. Dickheuer, M. Rasiński, A. Kreter and S. Brezinsek

Forschungszentrum Jülich GmbH - Institut für Energie- und Klimaforschung - Plasmaphysik, Partner of the Trilateral Euregio Cluster (TEC), 52425 Jülich, Germany

E-mail: s.ertmer@fz-juelich.de

Abstract. The erosion from plasma facing components (PFCs) has to be monitored in many kind of laboratory and fusion plasmas. For this purpose, spectroscopy is an essential tool. Under certain conditions the particle flux can be calculated from the absolute line intensities of the sputtered material using so-called S/XB-values.
The impact of light reflection on the emission induced by sputtered particles at the mirror-grade polished surface of tungsten (W) and aluminum (Al) was investigated in a low density ($n_e \approx 2 \times 10^{12}\,cm^{-3}$) and low temperature ($T_e \approx 3\,eV$) argon (Ar) plasma in the linear plasma device PSI-2 using high resolution spectroscopy. Using the line shape affected by Doppler shift we show that the light reflection has a considerable impact on the number of measured photons and has to be taken into account for calculating particle fluxes.
The Al target was sputtered by Ar ions at the incident ion energy of 120 eV. The measured profile of the Al I line (3961.52 Å) was compared with a Doppler-shifted emission model based on the Thompson energy distribution function. In this new model, the instrumental broadening and the impact of the Zeeman effect were also taken into account. The parameter for the high energy fall-off n of the energy distribution function ($\propto 1/E^{n+1}$), the surface binding energy E_b and the surface reflectance were derived by comparing the experimental and the synthetic spectrum.
The W target was sputtered by Ar ions at incident ion energies in the range of 30 eV to 160 eV. The influence of the ion impact energy on the energy distribution of the sputtered particles was demonstrated.

1. Introduction

Erosion of plasma facing components (PFC) is a natural process in laboratory plasma discharges, including magnetrons or hollow-cathodes but also in fusion plasmas. Specially in fusion research this topic is of a particular interest as the first wall and divertor have to withstand high particle and heat loads causing erosion [1]. Spectroscopy is an essential means for monitoring the particle flux into the plasma and provides the gross erosion. One way to calculate the flux is using the absolute intensity of characteristic lines emitted by the sputtered particles via so-called S/XB values [2]. For this purpose all possible effects influencing the measured intensities have to be assessed. Indeed, in fusion plasmas with divertor configurations the spectrometer observation angle is directed nearly perpendicular to the divertor surface. Existing investigations on light reflection in tokamaks with carbon PFCs show an effect of up to 20 % [3]. Metallic elements however, have a much higher reflectance. So, for instance, a mirror-polished W has a reflectance

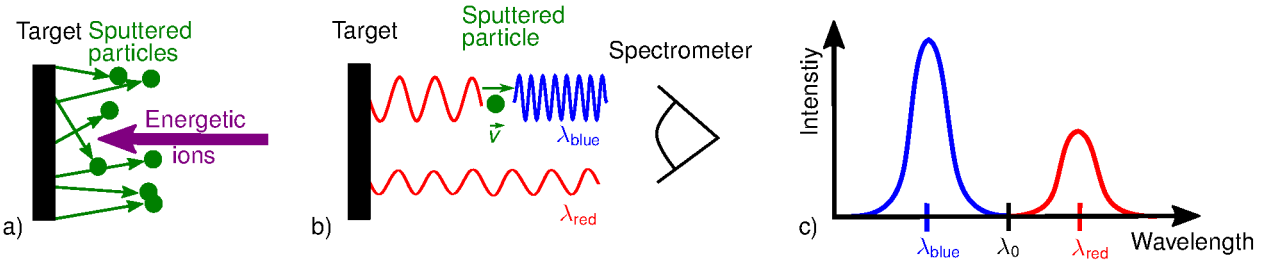

Figure 1. Schematic drawing of the method: a) the sputtering process, where the sputtered particles leave the surface with an angular and velocity distribution; b) the Doppler-shifted signal emitted by a sputtered atom with velocity v moving towards the detector along the surface normal is shown using the blue color. The signal after reflection at the target surface is shown using red color; c) the corresponding blue- and red-shifted components observed at the wavelengths λ_{blue} and λ_{red} in the spectrometer.

of $\approx 53\,\%$ in the visible range according to [4]. One expects, therefore, a much stronger effect of light reflectance on the detected emission of sputtered particles from metallic surfaces.
In this work the effect of light reflection induced changes in the line shape of sputtered atoms is investigated in details using the Doppler effect. Indeed, the Doppler effect governed by expression

$$\lambda = \lambda_0 \sqrt{\frac{c-v}{c+v}}, \tag{1}$$

allows to effectively distinguish the reflected from non-reflected component of emission. Here, λ is the detected and λ_0 is the emitted wavelength, c is the speed of light and v is the projection of the velocity of the emitting particle, e.g. the sputtered atom, on the line-of-sight. The principle of this method is shown in figure 1. Sputtered particles leave the surface with a certain velocity and angular distribution, they get excited in the plasma by electron impact excitation and emit photons isotropically (figure 1 a). Under an observation angle parallel to the target normal, light which is emitted with a component in movement direction is shifted to shorter wavelengths (blue-shifted) and can be detected directly with a high resolution spectrometer. Light emitted in the opposite direction is shifted to longer wavelengths (red-shifted) and can only be detected after reflection at the target surface (figure 1b). As a consequence, the two components separated by the Doppler shift in the spectrum can serve as a measure of the target's reflectance (figure 1c). A similar method was used in plasma conditions with much lower ionization degree for *in-situ* reflectance measurements with fast hydrogen atoms [5]. Moreover, the line shape can further be used to determine the angular and energy distribution of the sputtered particles testing the theoretical models and calculations from the codes such as TRIM [6] or SRIM [7].

2. Experimental setup

Experiments were performed at the linear plasma device PSI-2 described in details elsewhere [8]. A schematic top view of the spectroscopic setup is shown in figure 2a. The plasma column in PSI-2 has a symmetrical hollow profile. Mirror grade polished quadratic Al and W targets with a plasma-facing surface of were exposed to the density and temperature maximum of an argon plasma using the side manipulator. The target of W was chosen as fusion relevant PFC whereas Al target was chosen since it has a high reflectance in the range of visible light. Further, due to its lighter atomic mass the Doppler shift is more pronounced. Therefore, the Al experiment serves as a proof of principle. The Al target has been exposed over a long time in the plasma to observe *in-situ* the degradation the reflection degree. Plasma parameters in the maximum as

measured by the Langmuir probe have an electron temperature (T_e) of approximately 3 eV and an electron density (n_e) of 2×10^{12} cm^{-3}, like shown in figure 2b. Due to water cooling the target temperature during exposure was around 30 °C. The Ar^+ ions were accelerated onto the target by biasing the target to different mono-energetic impact energies from values corresponding to the floating potential up to 160 eV.
A high resolution echelle spectrometer in Littrow arrangement with a wavelength resolution of $\frac{\lambda}{d\lambda} \approx 7 \cdot 10^5$ was used to detect the light emitted by the sputtered particles via optical fiber coupling. Two spectra were studied at the same time: one spectrum was observed parallel (0°) and another one was observed perpendicular (90°) to the surface normal. The lines-of-sight are in the equatorial plane of the PSI-2. The line-of-sight at 0° was adjusted through the cathode onto the target and the line-of-sight at 90° was focused at a distance closer than 5 mm in front of the target. The back side illumination resulted in a spot size of ≈3-4 mm for both lines-of-sight. Spectral calibration, e.g. the calculation of the instrumental broadening and the dispersion was done by fitting emission spectra of reference hollow-cathode lamps of Al and W using the Voigt profile. We use the Al I line at 3961.52 Å and the W I line at 4982.59 Å [9]. Both lines are strongly populated during the sputtering process, as shown for instance in [10, 11]. In addition to the Al and W lamps, the lamps of Cr (Cr I line at 3963.68 Å [9]) and Ni (Ni I lines at 4980.16 Å and 4984.13 Å [9]) were utilized for measurements of dispersion. In contrast to measurements in a fusion plasma, the magnetic field of approximately 0.1 T is relatively weak at the target position in PSI-2. Under these conditions the ionization length is in the order of 10 cm leading to insignificant prompt re-deposition and recombination. Therefore the only source of emission of sputtered atoms in PSI-2 is limited to the direct excitation by electron impact.

3. Experimental results and analysis

The detected Al I spectra at both lines-of-sight are shown in figure 3. The spectrum observed at 90° (parallel to the target) is symmetric relative the central wavelength (dashed line), whereas in the line shape of the spectrum recorded at 0° two peaks, one shifted to shorter and one to longer wavelengths, are clearly visible. The thin black line shows the light emitted by a hollow-cathode lamp being used for spectral calibration. The broadening in the line shape detected at

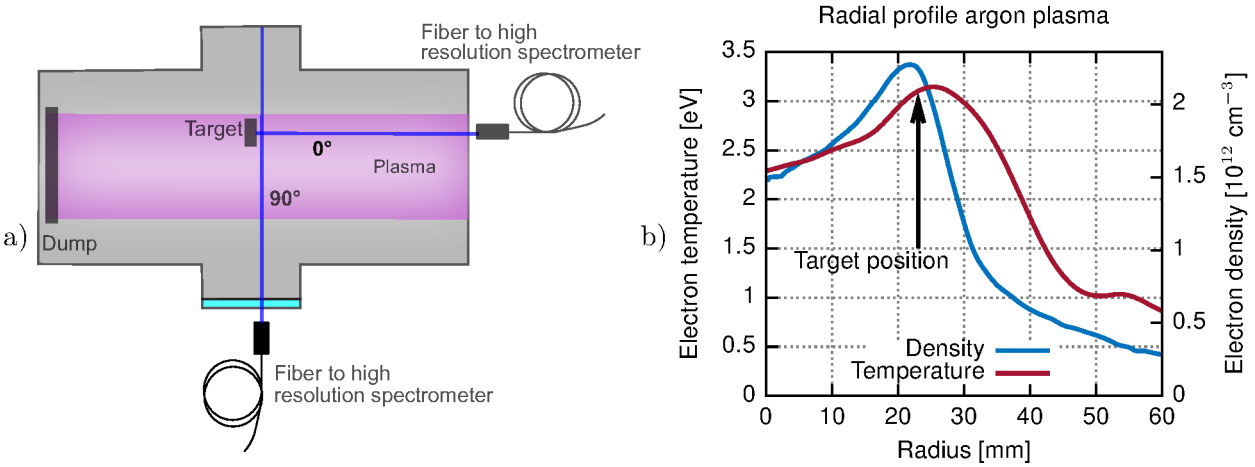

Figure 2. a) Schematic experimental setup at PSI-2: the target is exposed to the plasma and the sputtered atoms are observed via a parallel and a perpendicular line of sight using a high resolution spectrometer. b) Electron density and temperature profile during the experiment in PSI-2 as measured by Langmuir probe.

90° is caused by the angular and energy distribution of the sputtered atoms. At the condition of normal incidence one detects the same contribution of blue- and red-shifted photons. In the spectrum measured under 0° two maxima are observed. A strong intensity maximum is shifted to shorter wavelength, one less intense maximum is shifted to longer wavelength. The light from the blue-shifted component results from sputtered particles flying in the direction of detection. The red-shifted component can only be explained by light emitted in the direction of the target, which is detected only after being reflected at the target surface. Because of the interaction with the surface the red-shifted component is less intense.

In order to exemplify the effect of reflectance in the line shape of sputtered particles, we exposed the Al target for one hour to an argon plasma at an impact energy of the incoming ions of 120 eV. In figure 4 the first spectrum of the exposure is compared to the spectrum after one hour exposure. The change from specular reflectance to diffusive reflectance is evident from the intensity decrease of the red-shifted component. Both spectra are normalized to their respective maximum, which is equivalent to the peak of the blue-shifted component. The spectrum after one hour shows a strong decrease of the ratio in between the reflected and non-reflected proportion. The only physical explanation for this effect is degradation of the reflectance, which is clearly visible in the pictures in figure 4. Here the polished target before the exposure and the blackened target after the exposure in PSI-2 are shown. In order to check if the blackening of the target was caused by oxidation after exposure, energy-dispersive X-ray spectroscopy and scanning electron microscopy was used to study the surface. These techniques showed an increased surface roughness in the order of a few hundred nanometer after exposure but no oxidation.

The high resolution spectra of sputtered Al I can be used to derive not only the reflectance of the surface, but also the characteristics of the energy distribution of sputtered particles. Moreover, even though in many cases the reflectance of photons at a surface is disadvantageous

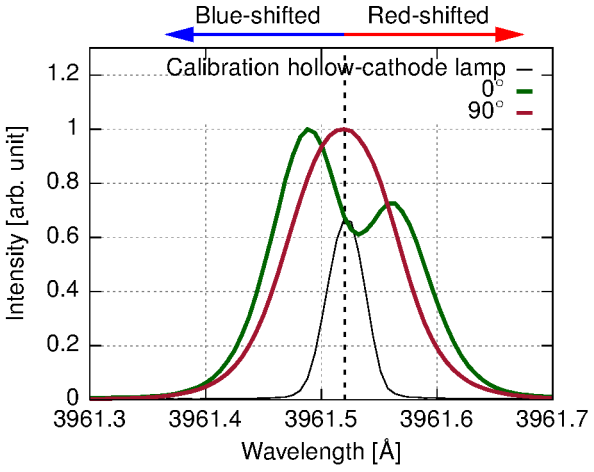

Figure 3. Detected Al I line shape observed perpendicular and parallel to the target surface, while exposing Al target. The blue- and the red-shifted components are clearly pronounced in the line shape at the observation angle 0° relative to the normal. The dashed line symbolizes the central wavelength.

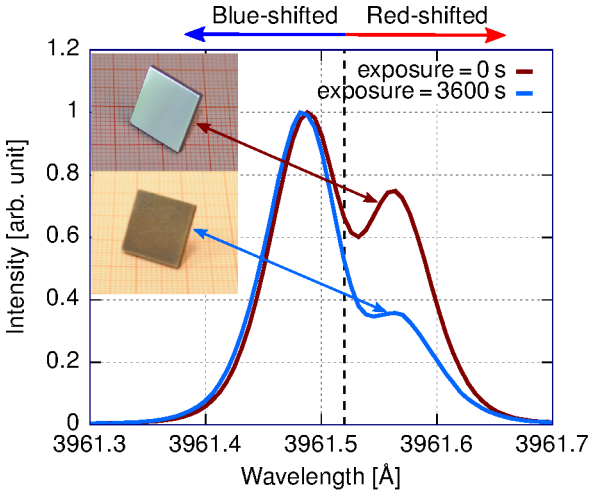

Figure 4. Emission spectrum of sputtered Al atoms at the beginning of the exposure and after one hour in an argon plasma under 100 eV ion impact energy. The decrease in the red-shifted component is caused by the surface roughness of the target. The polished bulk Al target before the exposure in the plasma is shown on the top left and the blackened target after one hour exposure below.

to determine the plasma parameter [12], here the high resolution spectroscopic data utilize this effect to limit the possible values for the surface binding energy E_b as exemplified below.
The Thompson energy distribution function $f(E)$ [13] given by the following expression

$$f(E) = \frac{E}{(E+E_\mathrm{b})^{n+1}} \left(1 - \sqrt{\frac{E_\mathrm{b}+E}{E_\mathrm{max}}}\right) \tag{2}$$

with $n = 2$ approximates the general behavior of the sputtered atoms in the whole energy range[1]. Here, E is the energy and E_{max} is the maximum recoil energy of sputtered atoms. The angular distribution is usually taken in the form $\cos^b(\theta)$, where θ is the polar angle and b is the power of the cosine. The cosine ($b = 1$), over- ($b > 1$), under- ($b < 1$) or heart-shaped distributions are possible for different targets at the incident energy of the Ar^+ ions on the order of 100...300 eV [14, 15, 16]. In case of Al the distribution close to $b = 1$ were reported in [15, 17] compared to the heart-shaped in [16]. For the surface binding energy E_b of Al the variations are much stronger. The values between 1.4 eV and 5.5 eV were measured or calculated. Detailed discussion on values of the surface binding energy and its connection to the sublimation energy can be found for instance in [18, 14].
A new Doppler-shifted emission model for sputtered atoms based on the results [19] was applied to fit the line shape of the Al I emission spectrum. The model was further developed to take the instrumental width into account, which leads to a broadening of the separate components. Finally, the Zeeman effect was included to provide an accurate description for the dip between the direct and reflected signals at the unshifted wavelength. To describe the experimentally obtained Al I spectrum at the observation angle of 0° a fitting procedure was carried out. The

[1] We note that the distribution (2) is also used without factor $(1 - \sqrt{...})$ for $E \approx E_\mathrm{b}$ [21] or with a factor $(1 - ...)$ instead [20].

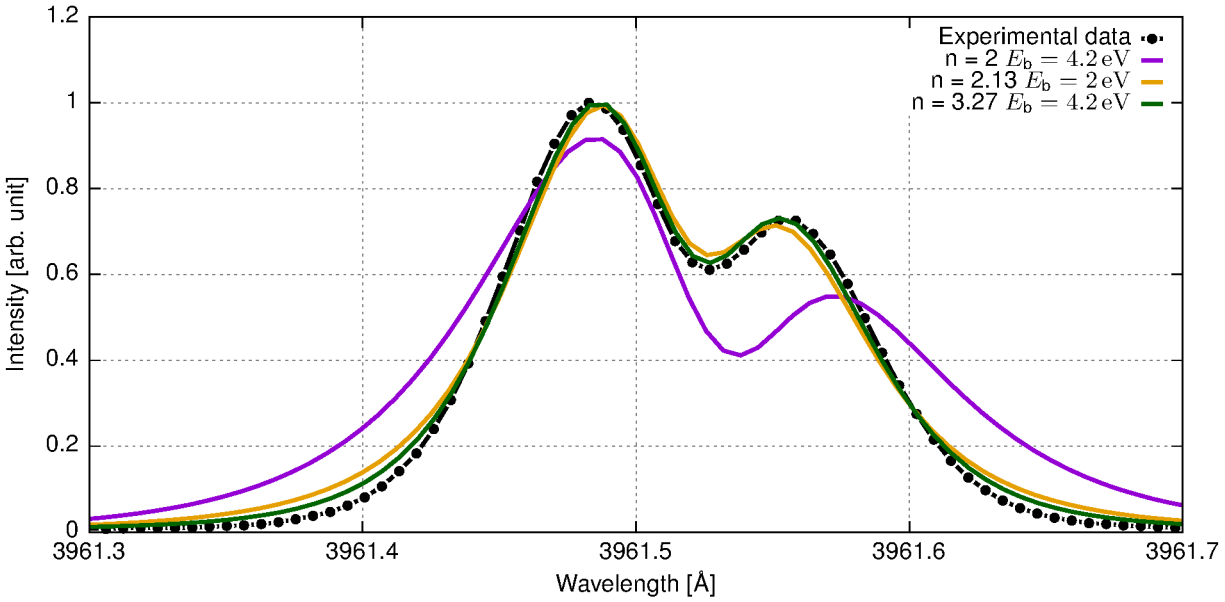

Figure 5. Experimental data at an observation angle perpendicular to the target compared to the model with different parameters: a standard Thompson energy distribution ($n = 2$, $E_\mathrm{b} = 4.2$ eV), with reduced binding energy and a fitted n ($n = 2.13$, $E_\mathrm{b} = 2$ eV) and the most accurate fit ($n = 3.27$, $E_\mathrm{b} = 4.2$ eV).

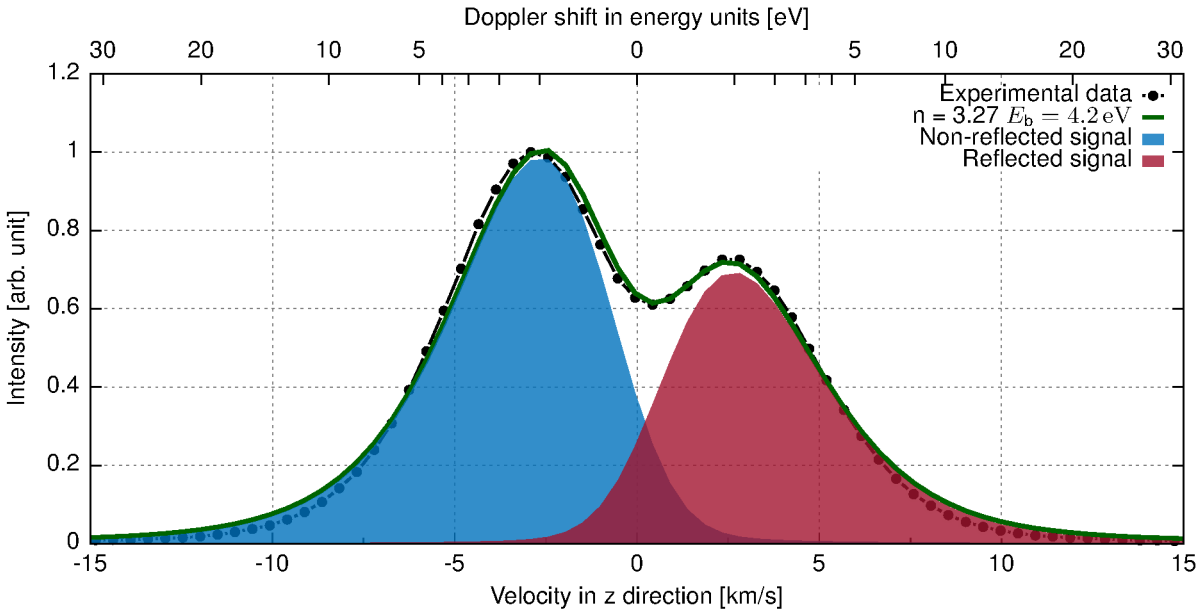

Figure 6. The fit of the Al I spectrum with $n = 3.27$ and $E_b = 4.2\,\text{eV}$ and its blue and red shifted component. The x-axis gives the velocity in the direction of the observer.

surface binding energy and the angular distribution are set manually, the parameter n and the intensities of the single components are obtained from a fit based on the before described Doppler-shifted emission model. Three different fits are shown in figure 5 and compared to the experimental data. For all these fits the angular distribution is assumed to be cosine, i.e. $b = 1$ in the normalized angular distribution function [19]. In a first attempt the standard Thompson energy distribution with fixed n set to 2 and E_b set to 4.2 eV is fitted to the experimental data and shown in purple. This describes the experimental data only poorly. The wings of the modeled spectrum are extremely broadened compared to the measured spectrum. The parameter n which is mainly responsible for the high energy tail in the energy distribution of the sputtered atoms thus has to be increased for low impact energy ions of 120 eV. The observed tendency reproduces practically the findings of the LIF measurements [20, 21]. The parameter n increases from $n = 2$ for incident ions with the energy of a few keV and reaches the values of $n \approx 3..4$ for energies down to 100 - 300 eV.

The yellow curve in figure 5 represents the fit of the parameter n with E_b set to 2 eV being close to the value of 1.8 eV found in [16]. This fit results in $n = 2.13$. The high energy tail is better described here compared to the standard Thompson distribution. It can be seen, however, that in this case the theoretical maxima are too close. Consequently, a higher E_b has to be chosen to increase the distance between the emission maxima. A parameter scan in E_b was carried out, for each set value of E_b n was obtained from the fit, and the most accurate description was found with E_b set to 4.2 eV and obtaining a fit of $n = 3.27$. These results are shown using the green line. The distance between two maxima and the high energy tail of the spectrum can be described reasonable well. We point out that this value is also in good agreement with the average surface binding energy of 4.2 eV as extracted from experiments by Stepanova in [14].

In figure 6 the components of emission are plotted over velocity and energy of sputtered atoms. The overlap of the components here is due to instrumental width as shown in figure 3. Finally, the value of reflectance taken from the integral of the red and the blue shifted component equals to 70 %. This is lower than for a mirror-like Al surface, but can be explained by the exposure time of one minute before recording the spectrum. The layer

with the thickness of about 150 nm which is $\lambda/3$ is removed during this time. As known that mirror-like properties of the surface are valid for irregularities on the order of $\lambda/10$ or less [22]. For investigating fusion-relevant PFCs the W target was exposed to the same conditions as the Al target. A higher atomic mass leads to lower velocities of the sputtered particles in the case of W, which in turn results in a weaker blue- and red-shifted component. Thus the effect of reflectance in the line shape is less pronounced, but still detectable as can be seen in figure 7. Here, instead, the influence of the ion impact energy on the energy distribution of sputtered W was investigated. Different bias voltages were applied to the target and spectra of the light emitted by the sputtered W were acquired. In figure 7 the spectra detected at the angle of 0° for different mono-energetic ion impact energies are displayed. With increasing ion impact energy a symmetric movement of blue- and red-shifted component is detectable: the blue-shifted component moves to shorter wavelength, whereas the red-shifted component moves to longer wavelength at the same extent. Also in this case the line shape depends on the particles' velocity as well as on their angular distribution. Assuming a constant angular distribution of the sputtered atoms in this energy range, a stronger shift of the peaks is equivalent to an increase in the sputtered particles' velocity. This means that, under the assumption of a constant angular distribution, the energy distribution of the sputtered W extends to higher values with increasing ion impact energies. These results are in qualitative agreement with ion beam experiments at higher impact energies of Goehlich [21].

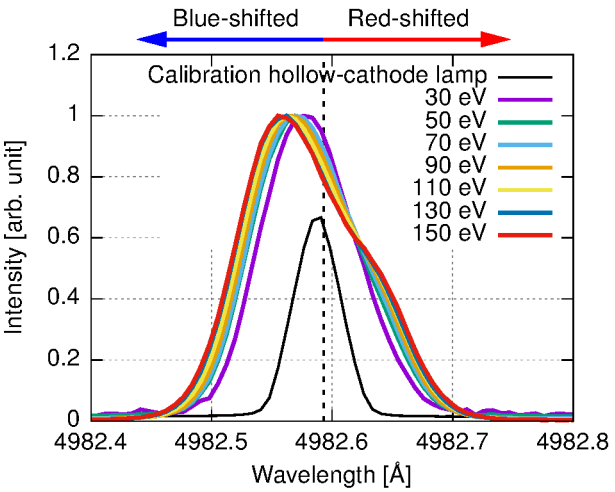

Figure 7. Emission spectrum of tungsten in an argon plasma for different ion impact energies. With increasing energy a symmetric movement of blue and red-shifted component is observed.

4. Conclusion and outlook

We show that the light reflection can be detected in the line shape of sputtered particles. The Doppler effect is less prominent for sputtered W than for lighter and thus faster Al. Therefore the effect of reflection degradation during plasma exposure is more pronounced. It is obvious that the reflected light at the material surface has to be taken into account for interpretation of the measured photon flux. This is especially important for fusion devices with metallic walls where the reflectance is much higher than for carbon machines.

The line shape of Al I was modeled to determine the reflectance of the surface. Furthermore, the model could be used to determine the energy distribution of the sputtered Al. It was found that the fitting parameter n of the Thompson energy distribution given by equation (2) for 120 eV ion impact energy has to be set to a value of 3.27. The surface binding energy was found to be 4.2 eV. For W it is shown that the energy distribution of sputtered atoms is depending on the impact energy of the incoming ions. With higher impact energy the sputtered atoms leave the surface with a higher energy. Future work aims at modeling the angular and energy distribution of sputtered W based on the line shape at different impact energies.

5. Acknowledgment

This work has been carried out within the framework of the EUROfusion Consortium and has received funding from the Euratom research and training programme 2014-2018 and 2019-2020 under grant agreement No 633053. The views and opinions expressed herein do not necessarily reflect those of the European Commission.

[1] R. Wenninger et al. *Nucl. Fusion* 57 046002 (2017).
[2] S. Brezinsek et al. *Phys. Scr.* T170 014052 (2017).
[3] N.H. Brooks et al. *J. Nucl. Mater.* **337** (2005) 227–231.
[4] W. S. M. Werner et al. *J. Phys Chem Ref. Data* **38** (2009) 1013-1092.
[5] S. Dickheuer et al. *Review of Scientific Instruments* **89**, 063112 (2018).
[6] W. Eckstein "Computer Simulation of Ion-Solid Interactions", Springer-Verlag (1991).
[7] J. F. Ziegler, "SRIM/TRIM code", see www.srim.org [2019, August 29].
[8] A. Kreter et al. *Fusion Science and Technology* **68** (2015) 8-14.
[9] A. Kramida, et al (2018). NIST Atomic Spectra Database (ver. 5.6.1) [Online] [2019, August 29].
[10] S. Ertmer et al. conference proceeding 45th EPS Conference on Plasma Physics (2018).
[11] H. Scheibner et al. *Rev. Sci. Instrum* **73** (2002) 378.
[12] B. Schunke et al. *Proc. 31st EPS Conf. on Plasma Physics (London, UK)* (2004) *28G (ECA)* P-4.111.
[13] M. W. Thompson *Phil. Mag.* **18** 377-414 (1968).
[14] M. Stepanova et al. *J. of Vacuum Science & Technology A* **19** (2001) 2805.
[15] J. Jorzick et al. *Appl. Phys. A* **78** 655–658 (2004).
[16] R. Ramos et al. *J. Phys. D: Appl. Phys.* **41** (2008) 152003.
[17] P. C. Smith et al. *J. of Vacuum Science & Technology A* **17** (1999) 3443.
[18] R.Behrisch and W. Eckstein "Sputtering by Particle Bombardment", Springer-Verlag (2007) 236, 246.
[19] S. Dickheuer et al. *Phys. Plasmas* **26**, 073513 (2019).
[20] H.L. Bay *Nucl. Instrum. Methods Phys. Res. B* **18** (1987) 430-445.
[21] A. Goehlich et al. *J. Nucl. Mater.* **266-269** (1999) 501-506.
[22] R. Shimizu *Appl. Phys.* **18** (1979) 425-426.